

Observation of an unexpected negative isotope shift in $^{229}\text{Th}^+$ and its theoretical explanation

M. V. Okhapkin,¹ D. M. Meier,¹ E. Peik,^{1,*} M. S. Safronova,^{2,3} M. G. Kozlov,^{4,5} and S. G. Porsev^{2,4}

¹*Physikalisch-Technische Bundesanstalt, Bundesallee 100, 38116 Braunschweig, Germany*

²*Department of Physics and Astronomy, University of Delaware, Newark, Delaware 19716, USA*

³*Joint Quantum Institute, National Institute of Standards and Technology and the University of Maryland, College Park, Maryland, 20742, USA*

⁴*Petersburg Nuclear Physics Institute, Gatchina 188300, Russia*

⁵*St. Petersburg Electrotechnical University LETI, St. Petersburg 197376, Russia*

(Received 13 May 2015; published 25 August 2015)

We have measured the hyperfine structure and isotope shifts of the 402.0- and 399.6-nm resonance lines in $^{229}\text{Th}^+$. These transitions could provide pathways towards the excitation of the ^{229}Th low-energy isomeric nuclear state. An unexpected negative isotope shift relative to $^{232}\text{Th}^+$ is observed for the 399.6-nm line, indicating a strong Coulomb coupling of the excited state to the nucleus. We have developed an all-order approach to the isotope shift calculations that is generally applicable to heavy atoms and ions with several valence electrons. The theoretical calculations provide an explanation for the negative isotope shift of the 399.6-nm transition and yield a corrected classification of the excited state. The calculated isotope shifts are in good agreement with experimental values.

DOI: [10.1103/PhysRevA.92.020503](https://doi.org/10.1103/PhysRevA.92.020503)

PACS number(s): 31.30.Gs, 31.15.A-

The existence of a low-energy nuclear isomeric transition in ^{229}Th [1–3] has stimulated the development of novel ideas and concepts in the borderland between atomic and nuclear physics [4,5], with conceivable applications such as nuclear clocks [6–10] and γ -ray lasers [11]. The wavelength of this very narrow nuclear transition is predicted to be 160(10) nm [2,3]. The big uncertainty in the transition wavelength, its location in the vacuum ultraviolet range, and the radioactivity of ^{229}Th with a half-life of about 7900 years present experimental difficulties that have so far prevented optical spectroscopy of the transition. A promising approach towards an excitation of the isomer is the use of electronic bridge or nuclear excitation by electron transition (NEET) processes [12–14] that involve finding sufficiently strong electronic transitions close to the nuclear resonance. The Th^+ ion, with its large density of states, offers a high probability of locating such electronic bridge pathways. Using the long-lived ^{232}Th isotope we have investigated two-photon excitation of electronic levels of Th^+ in the expected energy range of the isomer and have found 43 previously unknown levels [15].

A well-known influence of the nucleus on electronic spectra of atoms is the isotope shift (IS) that for heavy atoms is dominated by differences in the overlap of nuclear and electronic charge distributions, the so-called field shift (FS). Extensive studies of isotope shifts in the dense level schemes of Th and Th^+ have been performed [16–19], providing shifts of more than 350 excited states of $^{230}\text{Th}^+$ with respect to $^{232}\text{Th}^+$ [19]. In all but three cases, the shift of the excited state is smaller than that of the $6d^27s$ ground state (GS), indicating the smaller overlap of the excited electronic configuration with the nucleus for almost all states. Although a nearly complete compilation of the 15 lowest electron configurations is published [20], only very few low-energy excited states belonging to fs^2 and s^2p configurations with strong Coulomb

interactions with the nucleus are known in Th^+ . Such states will be of relevance for the implementations of electronic bridge or NEET processes.

Based on the laser spectroscopy of trapped ions, we present here measurements of the isotope shifts and hyperfine structure (HFS) of $^{229}\text{Th}^+$ for two of the strongest Th^+ resonance lines at 399.6 and 402.0 nm. A positive IS of the 402-nm line of $^{229}\text{Th}^+$ relative to $^{232}\text{Th}^+$ of 19 GHz has been reported already [18]. Unexpectedly, we observe a negative isotope shift (i.e., a lower transition frequency) of the $0_{3/2} \rightarrow 25\,027_{1/2}$ line at 399.6 nm with respect to $^{232}\text{Th}^+$, indicating a strong field shift of the excited state (states are labeled by their energy in cm^{-1} and the angular momentum J). Since the $25\,027_{1/2}$ state was previously identified as $5f6d^2$ [20], a negative isotope shift would contradict the available IS data for Th^+ , as discussed above.

Resolving this issue requires precision theoretical IS calculations. This is a difficult endeavor due to several factors: (1) Th^+ is a heavy trivalent system with electronic configurations containing $5f$ electrons that are very strongly correlated with core electrons; (2) there is a very large number of energy levels between the ground state and the $25\,027_{1/2}$ level (it is the 82nd odd level); and (3) the state of interest is very strongly mixed with nearby states, complicating the calculations and identification of the levels. Therefore, a very accurate and different approach is needed for the Th^+ IS calculation.

We have developed a method to calculate IS for multivalent heavy systems based on the hybrid approach that combines configuration interaction and all-order linearized coupled cluster methods (CI+all-order). While the CI+all-order method has been applied to calculating energies, transition properties, and polarizabilities [21–23], we implement it here for IS calculations. This is also an application of the CI+all-order method for such highly excited states of multivalent atoms for any system. An ability to accurately calculate IS for heavy ions opens a pathway for the accurate determination of nuclear radius differences between isotopes of heavy elements based on *ab initio* calculations.

*Author to whom correspondence should be addressed: ekkehard.peik@ptb.de

In our experiments we use a linear Paul trap, described in Refs. [15,24]. The trap is loaded with $\geq 10^5$ Th^+ ions by laser ablation from a dried $\text{Th}(\text{NO}_3)_4$ solution deposited on a tungsten substrate. Collisions with an argon buffer gas at 0.1 Pa pressure cool the ions to room temperature and quench the population of metastable states that are optically pumped by the laser excitation. Pulsed excitation of the $24\ 874_{5/2}$ and $25\ 027_{1/2}$ states is provided by a cw extended-cavity diode laser (ECDL) with an output power of 25 mW passing through a fast acousto-optical modulator. The excitation pulse duration is 70 ns and a pulse repetition rate of 1 kHz is adapted to the collisional quenching rate of about $\approx 1500/\text{s}$ [24]. Fluorescence of the excited Th^+ ions is detected using a photomultiplier (PMT). A fast gated integrator is used to evaluate the PMT signal during a detection window with a duration of about 75 ns. The signal is then integrated over several hundred pulses. A small fraction of the cw radiation of the excitation ECDL is coupled to a Fabry-Pérot interferometer used as a reference to measure frequency intervals. After loading of Th^+ we observe simultaneously the fluorescence signal from both ^{229}Th and ^{232}Th , indicating approximately equal abundances of both isotopes on the substrate. When it is necessary to avoid the influence of $^{232}\text{Th}^+$ ions, we apply an isotope-selective, resonantly enhanced, three-photon ionization to Th^{2+} [15] and eject these ions from the trap.

Determining the IS for ^{229}Th with a nuclear spin $I = 5/2$ requires knowledge of the HFS centroid frequency. The HFS of the $0_{3/2} \rightarrow 24\ 874_{5/2}$ transition of $^{229}\text{Th}^+$ at 402.0 nm consists of 12 lines with four components in each of the $\Delta F = -1, 0, +1$ branches, where F is the total angular momentum. We investigate the HFS by Doppler-free saturation spectroscopy and the excitation spectrum of both $^{229}\text{Th}^+$ and $^{232}\text{Th}^+$ isotopes is shown in Fig. 1(a). Figure 1(b) shows the HFS of $^{229}\text{Th}^+$ with high resolution. The width [full width at half maximum (FWHM)] of the resonances is ≥ 70 MHz and the width of the Doppler-broadened lines is ≈ 760 MHz. In Fig. 1(b), nine out of 12 possible resonances are resolved. The resonances caused by $F = 1 \rightarrow F' = 2$ and $2 \rightarrow 1$ transitions are overlapping within the width of the Lamb dips. The deformation of the Doppler shape caused by component $3 \rightarrow 2$ is also partially observable on the graph. The weak HFS component $4 \rightarrow 3$ is not observed due to the limited signal-to-noise ratio.

The HFS of the 399.6-nm line $0_{3/2} \rightarrow 25\ 027_{1/2}$ is shown in Fig. 2(a). The $25\ 027_{1/2}$ state of $^{229}\text{Th}^+$ consists of two components with $F = 2, 3$, therefore the HFS of the transition comprises six lines. The hyperfine components of $^{229}\text{Th}^+$ appear at frequencies below the position of the $^{232}\text{Th}^+$ line. To exclude a possible masking of a hyperfine component with the $^{232}\text{Th}^+$ Doppler-broadened line, we ejected $^{232}\text{Th}^+$ with the technique mentioned above. This experiment shows that there is no hyperfine component of the $^{229}\text{Th}^+$ overlapping with the $^{232}\text{Th}^+$ line. The saturation resonance of the transition $2 \rightarrow 3$ has a very weak intensity and is not observed in the experiment. The resonances caused by transitions $3 \rightarrow 3$ and $3 \rightarrow 2$ are resolved by scanning with a longer integration time [see the inset in Fig. 2(b)]. The dip in the middle correspond to a crossover resonance of V type with the common ground-state level $F = 3$ [see Fig. 2(b)].

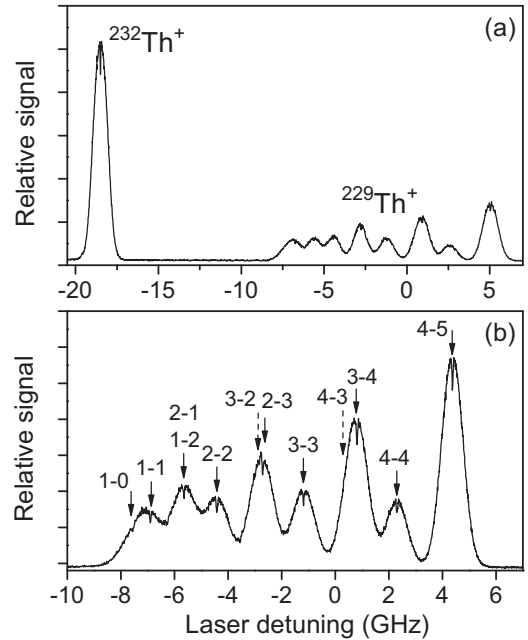


FIG. 1. (a) Fluorescence signal of the 402.0-nm line of $^{229}\text{Th}^+$ and $^{232}\text{Th}^+$ isotopes. (b) HFS signal of the 402.0-nm $^{229}\text{Th}^+$ line. The detuning counts from the recalculated HFS centroid position of the $^{229}\text{Th}^+$ isotope line. The components are labeled with the total angular momenta of lower and upper hyperfine levels. The dashed arrows in (b) show the recalculated positions of the $3 \rightarrow 2$ and $4 \rightarrow 3$ resonances.

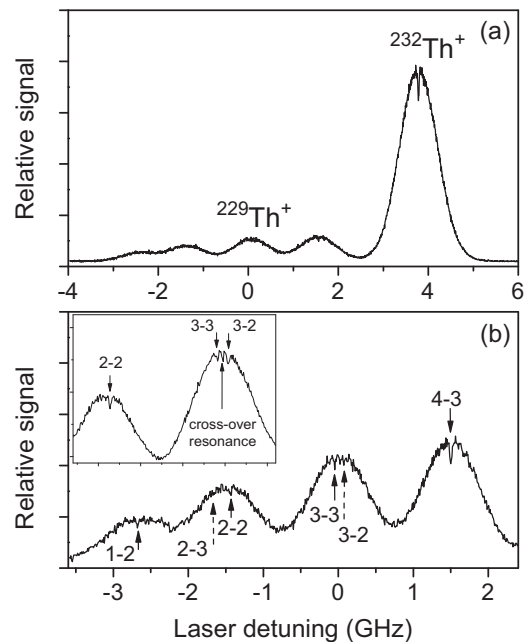


FIG. 2. (a) Fluorescence signal of the 399.0-nm line of $^{229}\text{Th}^+$ and $^{232}\text{Th}^+$ isotopes. (b) HFS signal of the 399.6-nm $^{229}\text{Th}^+$ line. The detuning counts from the recalculated HFS centroid position of the $^{229}\text{Th}^+$ isotope line, and the dashed arrows show the recalculated positions of the resonances $2 \rightarrow 3$ and $3 \rightarrow 2$. The inset shows resolved Doppler-free resonances of the components $3 \rightarrow 3$ and $3 \rightarrow 2$ and the V-type crossover resonance.

TABLE I. Hyperfine splitting factors of $^{229}\text{Th}^+$ electronic levels. The second row for the ground state shows the values obtained in Ref. [25].

Level (cm^{-1})	A (MHz)	B (MHz)	Reference
0	−444.2(3.4)	308(13)	This work
	−444.2(1.9)	303(6)	Ref. [25]
24 874	489.2(3.7)	−409(18)	This work
	488.9(3.7)	−413(16)	This work ^a
25 027	−45(19)		This work
	−42(16)		This work ^a

^aThese results represent the fit where the A and B parameters for the ground state are fixed to the values from Ref. [25].

In order to determine the hyperfine splitting factors A and B of the 402.0- and 399.6-nm lines, we measure the frequency intervals between the Lamb dips relative to the transmission peaks of the interferometer. For the 402.0-nm line the measured frequency intervals are fitted in a least-squares adjustment to determine the A and B factors for the ground and the $24\,874_{5/2}$ states. The algorithm attempts fits for all viable assignment combinations of F values for the nine resolved transitions shown in Fig. 1(b). The result is shown in Table I. The uncertainty results from inaccuracy of the measured frequency intervals, including a small contribution from the determination of the reference interferometer's free spectral range (FSR). The HFS factors for the ground electronic state (GS) in $^{229}\text{Th}^+$ are already known with high accuracy [25] (see Table I) and our results are in good agreement.

For the $25\,027_{1/2}$ state the B factor vanishes because of the absence of a quadrupole moment for $J = 1/2$. To determine the A factor of this level we fix the A and B values for the GS. We use the same algorithm to fit the frequency intervals between resolved transitions of this line. The uncertainty of the A value of the $25\,027_{1/2}$ state is determined by the accuracy of the frequency intervals and the uncertainty of the GS factors. Due to the weaker signal-to-noise ratio and smaller A factor of the excited state, the uncertainty of the fit is higher than that for the $24\,874_{5/2}$ state. Using the obtained values for A and B factors, we recalculate the position of the hyperfine components which are not observed. The calculated splitting of the HFS components $1 \rightarrow 2$ and $2 \rightarrow 1$ of the 402.0-nm line is 18 MHz, explaining the unresolved resonances of these lines. As a test of consistency, we calculate the complete shape of the saturation HFS spectra according to Ref. [26], fit it to the experimental signal, and find that it confirms the results presented above.

The IS of $^{229}\text{Th}^+$ is determined from the hyperfine centroid, corresponding to the position of the line for $A = B = 0$. For the 402.0-nm line, the centroid is ≈ 810 MHz red-detuned from the position of the $3 \rightarrow 4$ component. The isotope shift of $^{229}\text{Th}^+$ for this line is 18.86(7) GHz, in agreement with earlier, less precise measurements [17,18]. The uncertainty is determined by the precision of the frequency interval measurements and the calculated value of the HFS centroid. The GS of Th^+ yields a mixture of electronic configurations with leading components $6d^27s$ and $6d7s^2$ while the $24\,874_{5/2}$ level contains 26% $6d7s7p$ and 20% $5f6d^2$ [20]. For this transition the FS of the ground state is dominant [18] and determines the positive IS of the 402.0-nm line.

The 399.6-nm line shows a negative IS of $-3.67(5)$ GHz. The centroid of the line is shifted at ≈ 1.5 GHz to the lower frequency from the resonance $4 \rightarrow 3$ [see Fig. 2(a)]. The probability to observe a negative IS in Th^+ for a line originating from the GS was predicted to be very small [18] since the s electrons make the greatest contribution to the IS. For the odd-parity levels, a negative IS is observed only for the transition from the GS to the $8379_{7/2}$ level which has the leading electron configuration fs^2 . According to Ref. [20], the leading configuration of the $25\,027_{1/2}$ state is $5f6d^2$. The analysis in Ref. [16] indicates a weak FS for the $5f6d^2$ electron configuration, which means that the IS of the transition should be determined by the energy shift of the ground state which leads to a positive IS. A potential explanation for the negative IS would be a prior misidentification of the $25\,027_{1/2}$ level and the presence of a large admixture of a $7s^2nl$ configuration.

The field shift for isotope A' with respect to isotope A is defined as $\Delta\omega^{A',A} = K_{\text{FS}} \delta\langle r^{-2} \rangle^{A',A}$, where K_{FS} is the field shift constant and $\delta\langle r^{-2} \rangle^{A',A} = \langle r^{-2} \rangle^{A'} - \langle r^{-2} \rangle^A$. The FS operator H_{FS} is a one-particle operator which modifies the Coulomb potential inside the nucleus. We use the “finite field” method, which means that a perturbation is added to the initial Hamiltonian with the arbitrary coefficient λ , $H \rightarrow H_\lambda = H + \lambda H_{\text{FS}}$. We find eigenvalues E_λ by direct diagonalization of H_λ and then find the FS coefficient of an atomic level as [27]

$$K_{\text{FS}} = \frac{5}{6r_N^2} \frac{\partial E_\lambda}{\partial \lambda}, \quad (1)$$

where the nucleus is modeled as a homogeneously charged ball of radius r_N .

We use the CI+all-order method, with the modified Hamiltonian given above, to carry out the field shift calculation. All computations are repeated three times, with $\lambda = 0$ and $\lambda = \pm 0.01$. Then, Eq. (1) is used to evaluate the field shift constant. The general description of the CI+all-order method and its application to the calculation of energies, transition properties, and polarizabilities are given in Refs. [21–23]. We have modified the CI part of the method to be able to successfully generate much higher excited states than previously possible. This advancement will allow further applications of the CI+all-order method for highly excited states and systems with dense spectra. Another issue of the application of the CI+all-order method to IS is the requirement of very high numerical accuracy since the correction due to IS is small. Therefore, we improved and thoroughly tested the numerical accuracy of the approach, such as convergence of various iteration procedures.

While only ns orbitals have significant overlap with the nucleus, with $p_{1/2}$ having a much smaller overlap, other states will be affected by the inclusion of the IS effects due to the self-consistent nature of the potential. All of the ns orbitals become slightly less bound, leading to the expansion of the total self-consistent electronic potential. This in turn leads to changes of energies of the other states as they become more deeply bound in the modified potential. The IS of $6d$ and $5f$ electrons will be with the opposite sign of the $7s$ electron IS. One-electron estimates give the IS of the $5f$ electron being about 60% of the $7s$ IS with an opposite sign.

TABLE II. Comparison of the g factors and excitation energies (cm^{-1}) of Th^+ odd $J = 1/2$ states calculated using the CI+all-order method with experimental data compiled in Ref. [20] (see also Ref. [28]). The last column gives finite-size IS constants K_{FS} in GHz/fm^2 . All values are counted from the GS. The line printed in bold refers to the level studied in the experiment reported here.

State			g factor		Energy		K_{FS}
Ref. [20]	Calc.	J	Calc.	Expt.	Calc.	Expt.	Calc.
<i>5f6d7s</i>	<i>5f6d7s</i>	1/2	0.243	0.255	12390	11725	-82.1
<i>5f6d7s</i>	<i>5f6d7s</i>	1/2	0.558	0.523	14805	14102	-96.7
<i>5f6d7s</i>	<i>5f6d7s</i>	1/2	2.577	2.565	16207	15324	-65.9
<i>5f6d7s</i>	<i>5f6d²</i>	1/2	1.618	1.080	18307	17838	-120.4
<i>5f6d²</i>	<i>5f6d²</i>	1/2	0.405	1.007	19309	18568	-126.4
<i>5f6d7s</i>	<i>5f6d²</i>	1/2	0.730	0.770	23456	22355	-100.6
	+ <i>5f6d7s</i>						
<i>5f6d²</i>	<i>7s²7p</i>	1/2	0.568	0.600	25445	25027	5.8
	+ <i>6d7s7p</i>						
<i>5f6d²</i>	<i>5f6d²</i>	1/2	2.108	0.725	26024	25266	-119.7

The results of the CI+all-order calculation of the g factors and excitation energies of Th^+ odd $J = 1/2$ states are compared with experiment [20,28] in Table II. We find good agreement for the energy and g factor of the $25\,027_{1/2}$ level of interest. The last column gives differential finite-size IS constants K_{FS} in GHz/fm^2 for $J = 1/2$ levels, relative to the ground state. The table clearly demonstrates the opposite sign of the isotope shift constant for this level in comparison to the other states. Our calculations show $7s^27p$ with a contribution of 36% and $6d7s7p$ with 34% as the two dominant configurations for the $25\,027_{1/2}$ level, which explains the observations of the negative IS. Contributions from $6d^27p$ are 14% and from $5f6d^2$ 4% only. Using the value

$\delta\langle r^2 \rangle^{229,232} = -0.33(5) \text{ fm}^2$ [25,29] for the difference in the rms radii, we get -1.9 GHz for the CI+all-order IS of the 399.6-nm line, in good agreement with the experimental value of $-3.67(5) \text{ GHz}$. The difficulty of this particular calculation is the very large correlation correction for the $5f$ electrons and very strong configuration mixing for the $J = 1/2$ states. Our value for the 402.0-nm IS is 19.0 GHz , in excellent agreement with the experimental results of $18.86(7) \text{ GHz}$.

We have also carried out calculations using CI+many-body-perturbation theory (MBPT) [30] that was previously employed for IS calculations [31]. The CI+MBPT results for the 399.6- and 402.0-nm lines are 8.1 and 26.0 GHz, respectively, in very poor agreement with experiment. This demonstrates the success of the CI+all-order method and the need for the inclusion of the higher-order effects.

In summary, we have demonstrated that the CI+all-order method can accurately describe isotope shifts in such complicated systems as Th^+ . In turn, the IS measurements in actinides represent excellent benchmark tests for the development of these highly accurate theoretical methodologies. The results of this work are important for the selection of efficient transitions for the excitation of the ^{229}Th isomer, as the IS indicates the strength of the Coulomb interaction between electrons and nucleus that is relevant for NEET processes. The comparison of isotope and isomer shifts will give access to the Coulomb contribution to the nuclear transition energy, resolving a dispute about largely different theoretical predictions of the sensitivity of the nuclear transition frequency to the value of the fine-structure constant [32].

This work was supported in part by U.S. NSF Grant No. PHY-1404156 and Russian Foundation for Basic Research Grant No. 14-02-00241, and in part by EU FET-Open project 664732-nuClock.

-
- [1] R. G. Helmer and C. W. Reich, *Phys. Rev. C* **49**, 1845 (1994).
[2] B. R. Beck, J. A. Becker, P. Beiersdorfer, G. V. Brown, K. J. Moody, J. B. Wilhelmy, F. S. Porter, C. A. Kilbourne, and R. L. Kelley, *Phys. Rev. Lett.* **98**, 142501 (2007).
[3] B. R. Beck, C. Y. Wu, P. Beiersdorfer, G. V. Brown, J. A. Becker, K. J. Moody, J. B. Wilhelmy, F. S. Porter, C. A. Kilbourne, and R. L. Kelley, Lawrence Livermore National Laboratory, Internal Report No. LLNL-PROC-415170, 2009, <https://e-reports-ext.llnl.gov/pdf/375773.pdf>.
[4] S. Matinyan, *Phys. Rep.* **298**, 199 (1998).
[5] E. V. Tkalya, *Phys. Usp.* **46**, 315 (2003).
[6] E. Peik and Chr. Tamm, *Europhys. Lett.* **61**, 181 (2003).
[7] C. J. Campbell, A. G. Radnaev, A. Kuzmich, V. A. Dzuba, V. V. Flambaum, and A. Derevianko, *Phys. Rev. Lett.* **108**, 120802 (2012).
[8] W. G. Rellergert, D. DeMille, R. R. Greco, M. P. Hehlen, J. R. Torgerson, and E. R. Hudson, *Phys. Rev. Lett.* **104**, 200802 (2010).
[9] G. A. Kazakov, A. N. Litvinov, V. I. Romanenko, L. P. Yatsenko, A. V. Romanenko, M. Schreitl, G. Winkler, and T. Schumm, *New J. Phys.* **14**, 083019 (2012).
[10] E. Peik and M. Okhapiin, *C. R. Phys.* **16**, 516 (2015).
[11] E. V. Tkalya, *Phys. Rev. Lett.* **106**, 162501 (2011).
[12] E. V. Tkalya, V. O. Varlamov, V. V. Lomonosov, and S. A. Nikulin, *Phys. Scr.* **53**, 296 (1996).
[13] F. F. Karpeshin, I. M. Band, and M. B. Trzhaskovskaya, *Nucl. Phys. A* **654**, 579 (1999).
[14] S. G. Porsev, V. V. Flambaum, E. Peik, and Chr. Tamm, *Phys. Rev. Lett.* **105**, 182501 (2010).
[15] O. A. Herrera-Sancho, N. Nemitz, M. V. Okhapiin, and E. Peik, *Phys. Rev. A* **88**, 012512 (2013).
[16] G. L. Stukenbroeker and J. R. McNally, Jr., *J. Opt. Soc. Am.* **43**, 36 (1953).
[17] E. A. VERNYI and V. N. Egorov, *Opt. Spectrosc.* **6**, 170 (1959).
[18] E. A. VERNYI and V. N. Egorov, *Opt. Spectrosc.* **9**, 367 (1960).
[19] R. Engleman and B. A. Palmer, *J. Opt. Soc. Am. B* **1**, 782 (1984).
[20] R. Zalubas and C. H. Corliss, *J. Res. Natl. Bur. Stand., Sect. A* **78**, 163 (1974).
[21] M. S. Safronova, M. G. Kozlov, W. R. Johnson, and D. Jiang, *Phys. Rev. A* **80**, 012516 (2009).
[22] M. S. Safronova, V. A. Dzuba, V. V. Flambaum, U. I. Safronova, S. G. Porsev, and M. G. Kozlov, *Phys. Rev. Lett.* **113**, 030801 (2014).

- [23] M. S. Safronova, U. I. Safronova, and C. W. Clark, *Phys. Rev. A* **90**, 032512 (2014).
- [24] O. A. Herrera-Sancho, M. V. Okhapkin, K. Zimmermann, Chr. Tamm, E. Peik, A. V. Taichenachev, V. I. Yudin, and P. Głowacki, *Phys. Rev. A* **85**, 033402 (2012).
- [25] W. Kälber, J. Rink, K. Bekk, W. Faubel, S. Göring, G. Meisel, H. Rebel, and R. C. Thompson, *Z. Phys. A: At. Nucl.* **334**, 103 (1989).
- [26] J. Bordé and Ch. J. Bordé, *J. Mol. Spectrosc.* **78**, 353 (1979).
- [27] V. A. Korol and M. G. Kozlov, *Phys. Rev. A* **76**, 022103 (2007).
- [28] <http://web2.lac.u-psud.fr/lac/Database/Tab-energy/Thorium/Th-el-dir.html>
- [29] I. Angeli and K. P. Marinova, *At. Data Nucl. Data Tables* **99**, 69 (2013).
- [30] V. A. Dzuba, V. V. Flambaum, and M. G. Kozlov, *Phys. Rev. A* **54**, 3948 (1996).
- [31] J. C. Berengut, V. V. Flambaum, and M. G. Kozlov, *Phys. Rev. A* **73**, 012504 (2006).
- [32] J. C. Berengut, V. A. Dzuba, V. V. Flambaum, and S. G. Porsev, *Phys. Rev. Lett.* **102**, 210801 (2009).